Construction of synthetic ocean wave series along the Colombian Caribbean Coast: A wave climate analysis

Article *in* Applied Ocean Research · March 2016

Impact Factor: 1.29 · DOI: 10.1016/j.apor.2016.01.004

4 authors:

Andrés Fernando Osorio

National University of Colombia

54 PUBLICATIONS **312** CITATIONS

SEE PROFILE

Rubén Darío Montoya

Universidad de Medellín

3 PUBLICATIONS **0** CITATIONS

SEE PROFILE

Juan Carlos Ortíz

Universidad del Norte (Colombia)

19 PUBLICATIONS **63** CITATIONS

SEE PROFILE

Daniel Santiago Pelaez

Ensenada Center for Scientific Research an…

6 PUBLICATIONS **2** CITATIONS

SEE PROFILE

Applied Ocean Research 56 (2016) 119–131

Contents lists available at ScienceDirect

Applied Ocean Research

journal homepage: www.elsevier.com/locate/apor

Construction of synthetic ocean wave series along the Colombian Caribbean Coast: A wave climate analysis

Andrés F. Osorio [a,*], Rubén D. Montoya [b,a], Juan Carlos Ortiz [c], Daniel Peláez [a]

[a] OCEANICOS Research Group, Universidad Nacional de Colombia, Sede Medellín, Colombia
[b] GICI, GICAMH Research Groups, Universidad de Medellín, Medellín, Colombia
[c] Geosciences Area, Physics Department, Universidad Del Norte, Barranquilla, Colombia

ARTICLE INFO

Article history:
Received 13 April 2015
Received in revised form
23 November 2015
Accepted 5 January 2016

Keywords:
Waves
Synthetic series
Caribbean Sea
Hurricane waves
Colombia

ABSTRACT

In this paper a methodology is applied to generate synthetic wave series during mean and extreme conditions. An analysis is carried out that describes mean and extreme wave behavior for several climatic conditions along the Colombian Caribbean Coast. During mean conditions, the most energetic ocean waves are observed during the DJF season for both ENSO phases (El Niño and La Niña) for most of the Caribbean Sea. During the Niño years, there is a reduction in the speed of the north-east trade winds and their associated waves, but only in the DJF and MAM seasons. However, during the JJA season, this situation is reversed with the highest values occurring during El Niño and low values appearing during La Niña. Toward the east around the Guajira region, this general pattern is shown to change significantly. For extreme conditions, the results show a significant influence of extreme events toward the northwest, around La Guajira and the insular zones of San Andres and Providence when compared with other regions along the coast. All of these results (including the synthetic wave series) provide a design and management tool for the successful implementation of any coastal project (scientific or consulting) in Colombia.

1. Introduction

The world's climate is very changeable. This affects the conditions in coastal areas, impacting engineering applications like port design and industries like fishing and tourism. Issues such as sediment transport and erosion can vary along a specific coastal area.

For the Colombian Caribbean Sea, the relationship between large scale climatology and ocean waves is still not properly understood. This problem is combined with a lack of highly accurate long-term information. The wave climate information currently available is still limited, as it is based on visual observations and therefore does not have a suitable spectral, spatial and temporal resolution. Furthermore, information is not present for extreme conditions. Information from agencies that monitor the climate is available, but some of it does not contain all of the wave parameter details or a high enough resolution for specific coastal areas. Although the wave information provided by satellites allows for the observation of vast areas, it does not permit high temporal resolution data to be obtained for a given point (two data values every 10 days) or the directional wave spectrum to be estimated. The number of buoys moored in deep water near the Colombian coast per kilometer of shoreline is very poor when compared to the number of buoys in the waters of other countries. As a result, repercussions have emerged from an engineering and scientific point of view, such as inadequate designs of coastal structures, poor understanding of coastal dynamics and even loss of human life, among many other issues.

The above information highlights the importance of this research for the Colombian Caribbean coastal area, considering that Colombia has eight main port zones, seven of which are found on the Caribbean coast. These ports handle ninety percent (90%) of the country's imports and exports. The principle mainland ports and tourism areas are located in La Guajira, Santa Marta, Barranquilla, Cartagena and the insular region of San Andres and Providence, which along with the other cities that form part of the Caribbean, produce about 16% of the country's gross national product (GNP). In terms of biodiversity, the Colombian Caribbean has more species than other regions of the country.

Due to the lack of wave information with the required temporal and spatial resolution in the Colombian Caribbean, it is necessary to resort to other sources of data. One possibility is to use synthetic or modeled data, obtained through numerical models that employ wind fields from the past, which can obtain wave information by using reanalysis techniques (Hindcast). These types of analyses have been previously developed for specific cases in the

* Corresponding author at: Universidad Nacional de Colombia, Sede Medellin, Carrera 80N° 65-223 (Bloque M2). Of 209, Medellín, Colombia. Tel.: +57 4 4255142: fax: +57 4 4255100.
E-mail address: afosorioar@unal.edu.co (A.F. Osorio).

0141-1187/$ – see front matter © 2016 Elsevier Ltd. All rights reserved.
http://dx.doi.org/10.1016/j.apor.2016.01.004

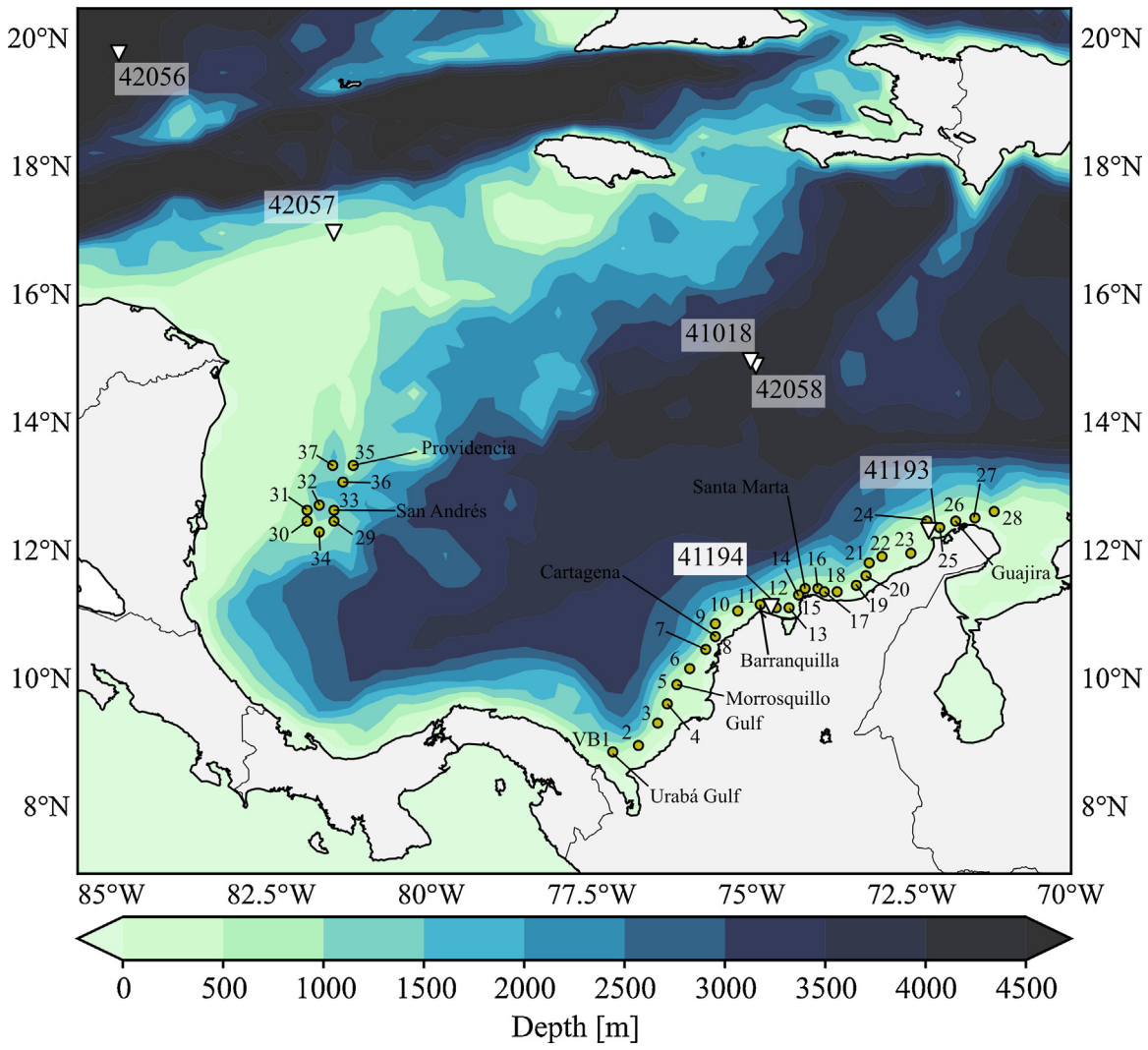

Fig. 1. Location of the virtual buoys (VBs): instrumental buoys used for calibration and validation and to provide bathymetric information for the Caribbean Sea.

Colombian Caribbean, for both mean fields [1–4] and extreme fields [5–7]. However, such approaches do not set modeling parameters that include the physical process of each condition in order to integrate time series data. Furthermore, they do not investigate the behavior of ocean waves along the Colombian Caribbean coast as whole. Around the world, several authors have performed wave climate analysis based on numerical models [8–13], among others.

Large-scale phenomena such as the El Niño/Southern Oscillation (ENSO), among others, affect the characteristics of the Colombian Caribbean climate on different spatial and temporal scales, which includes short-term extreme events such as hurricanes. Therefore, it is necessary to apply new knowledge and technology currently available to reconstruct a historical wave database for the Colombia Caribbean based on numerical modeling that considers the dynamics of interactions between the atmosphere and the ocean for these climatic conditions. The aim is to provide the necessary information to carry out research, develop infrastructure and make reliable decisions regarding coastal and ocean areas. This paper is organized as follows: Section 2 presents a description of the study area, Section 3 gives a description of the general methodology and the data employed, including a description of the blended methodology and calibration process, Section 4 performs a comprehensive analysis of wave climate along the coast, and the last section gives the summary and conclusions.

2. Study area

Since the main aim of this study was to construct reliable wave data for engineering applications in the Colombian Caribbean, 37 sites for Virtual Buoys (hereafter VBs) along a belt that encompasses the whole coastline including the island of San Andres were selected (Fig. 1). This allowed information to be generated close to urban centers of interest, and at the same time achieved an adequate coverage of the coast with a maximum separation of approximately 65 km between the VBs. VBs were selected in deep waters, between 100 and 200 m in depth (oceanic criterion for typical wave periods in the Colombian Caribbean) and the number (37) of VBs was sufficiently dense to obtain reliable reference information from the most important sites of interest along the coast.

Some authors [14,15] describe four climatic seasons in the Caribbean Sea: the main dry season December–January–February (DJF), the secondary wet season March–April–May (MAM), the brief dry season known as the “veranillo” June–July–August (JJA) and the main wet season September–October–November (SON). However, it is valid to talk about only two main climatic periods: (i) the dry season and (ii) the wet season. The dry season is from December to April and is characterized by low precipitation and the predominance of synoptic wind (or trade winds) that blow from the north/northeast. The rainy (or wet) season covers the period from

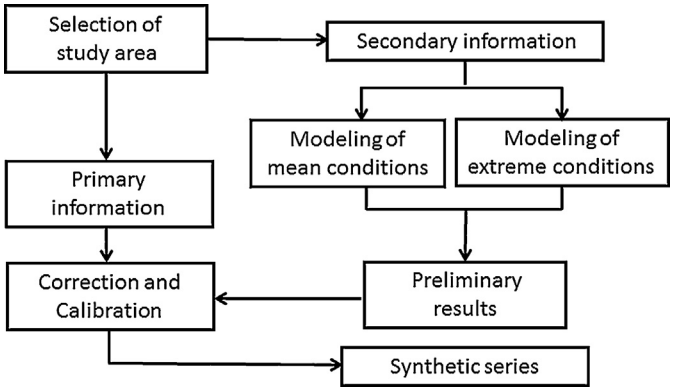

Fig. 2. General diagram of the proposed methodology.

May–November. This season has the highest precipitation (an average of 125.7 mm) and relatively weak winds blowing from north to south until August. This climatic seasonality is typical of the southern part of the Caribbean Sea and is caused by the oscillations of the Inter-Tropical Convergence Zone (ITCZ) [16]. The seasonal contrast is important for tourism, water resource allocation, hydrological considerations and maritime activities, among other factors.

However, this dry/wet regime only broadly defines the climate of the region, as orography and elevation are significant modifiers on a sub-regional scale. The region under study is one of complex and diverse topography that includes continental territories, island chains and mountain ranges of varying orientations and elevations. Tropical storms and hurricanes are seasonally common in the Caribbean and merit brief discussion as they cause significant loss of life, extensive infrastructural damage and disruption to Central American and Caribbean economies and ways of life. On average, eight hurricanes pass near or through the Caribbean region each year, but this number can vary significantly from year to year. Global climatic phenomena such as the El Niño Southern Oscillation (ENSO) seem to play a role in determining the number of storms which will develop and pass through the Caribbean. During the warm phase, there is an apparent decrease in the frequency of tropical storms due to an increase in wind shear in the Caribbean during the hurricane season. There is also evidence of decadal variation in storm activity, with some decades on average being less active (1970s to 1990s) than others (1920s to 1960s) [17,18]. The hurricane season runs from June to November with a peak in activity in September. The significant wave height can be magnified by polar fronts [19] during the first three months of the year and the passage of storms and hurricanes between June and November [7].

3. Methodology and data

Based on previous local methodologies [1,2,5; among others] and international validation approaches [3,4], this paper proposes a methodology to generate synthetic wave series during mean and extreme conditions. This allows both a mean and extreme series to be constructed, which can later be consolidated into one single data series. The time series obtained are employed to research the wave climate along the coastal areas in the Colombian Caribbean sea. A diagram of the proposed methodology is presented in Fig. 2. The methodology involves 5 general steps. Step 1 is to choose the study area. Step 2 is to gather the base information to feed into the model. Step 3 is to run the wave models on an oceanic scale in the Caribbean Sea (with mean and extreme conditions), and then to downscale the results to the detailed virtual buoys using nested or regular grid runs (based on the calibration process). Step 4 is to use primary information (satellite data and buoys) to correct (if necessary) and validate the preliminary series. The correction and comparison is made in the probability domains. Both simulated and satellite series are plotted (in a Q-QPlot) and a linear adjustment between them is carried out for analysis in the probability domains. The validation is also carried out in the same way but with instrumental *in situ* buoy data. Finally, Step 5 is to generate the coupled synthetic series for mean and extreme fields.

The selection of the base information is a crucial step for the construction of any numerical model as its accuracy and reliability dictates the quality of the results obtained. The detailed description to obtain the extreme and mean time series of the main wave parameters is described as follows.

3.1. Mean wave field generation

As the main forcing, winds at a height of 10 m were taken from the North American Regional Reanalysis (NARR) database [20]. The grid resolution is 349 × 277, which was approximately 0.3 degrees (32 km) at the lowest latitude. The three-hourly zonal and meridional wind components from 1979 to 2012 were bilinearly interpolated to a resolution of 0.25° × 0.25° (in the domain of −89.0 to −65.0 in longitude and 7.0–20.0 in latitude), and employed as a forcing of the wave model. Compared to the NCEP's global reanalysis database, NARR has better adjustments to wind measurement stations and employs advances in land–atmosphere interaction. These improvements make NARR a consistent and high-resolution reanalysis project, ideal for the Caribbean region [1]. Bathymetries were taken from the ETOPO1 model (http://www.ngdc.noaa.gov/mgg/global/global.html) [21]. Waves measured from the records of two Direccion General Maritima (DIMAR) *in situ* buoys located near the Colombian Caribbean coast (Table 1 – available at the National Data Buoy Center (http://www.ndbc.noaa.gov/)) and Satellite data from the GlobWave project (www.globwave.org) were employed to calibrate and validate the model for mean conditions. Satellite data is held by the French institute IFREMER (Institut Français de Recherche pour l'exploitation de Mer). GlobWave has altimetry products (significant wave height, Hs) which fuse the trajectories of several missions, with approximately 30 years of data.

To generate three-hourly time series of the main wave fields for mean conditions, the third generation (3G) SWAN (Simulating Waves Nearshore) model, developed by the Delft University of Technology [22,23] was employed. The SWAN model allows the propagation of complete wave series and considers wind as a forcing to calculate the balance of wave energy. The model is effective when direction and wind speed change suddenly, so is very useful for areas near the coast [24].

The main settings and quality tests of the model are: propagation in two spatial directions, "x" and "y", a direction space θ and a frequency space ω, and a constant sea level. Based on the information mentioned above and oceanic conditions in the Caribbean Sea, the variation in the tide is considered insignificant and the energy flows coming from the north and east Atlantic through the Greater and Lesser Antilles are not considered. Wave–current interactions were not considered given the strong increase in the time simulation and the low contribution to the quality of modeled ocean waves [25].

Several tests were performed using nested grids, full grids and all the parameterizations included in the SWAN model (results not shown here). The main goal was to find the best behavior of the model based on simulation time and the quality of the ocean waves obtained (modeled against DIMAR buoys). The best results were obtained for a regular grid with a resolution of $\Delta x = \Delta y = 1/10°$. The computational grid area extends from −89.0° to −65.0° in longitude and from 7.0° to 20.0° in latitude. The numbers of nodes of the computational grid are 241 (x) and 131 (y). The model was run in non-stationary two-dimensional mode. The spectral and directional resolution applied was 30 frequencies, varying from 0.03 Hz

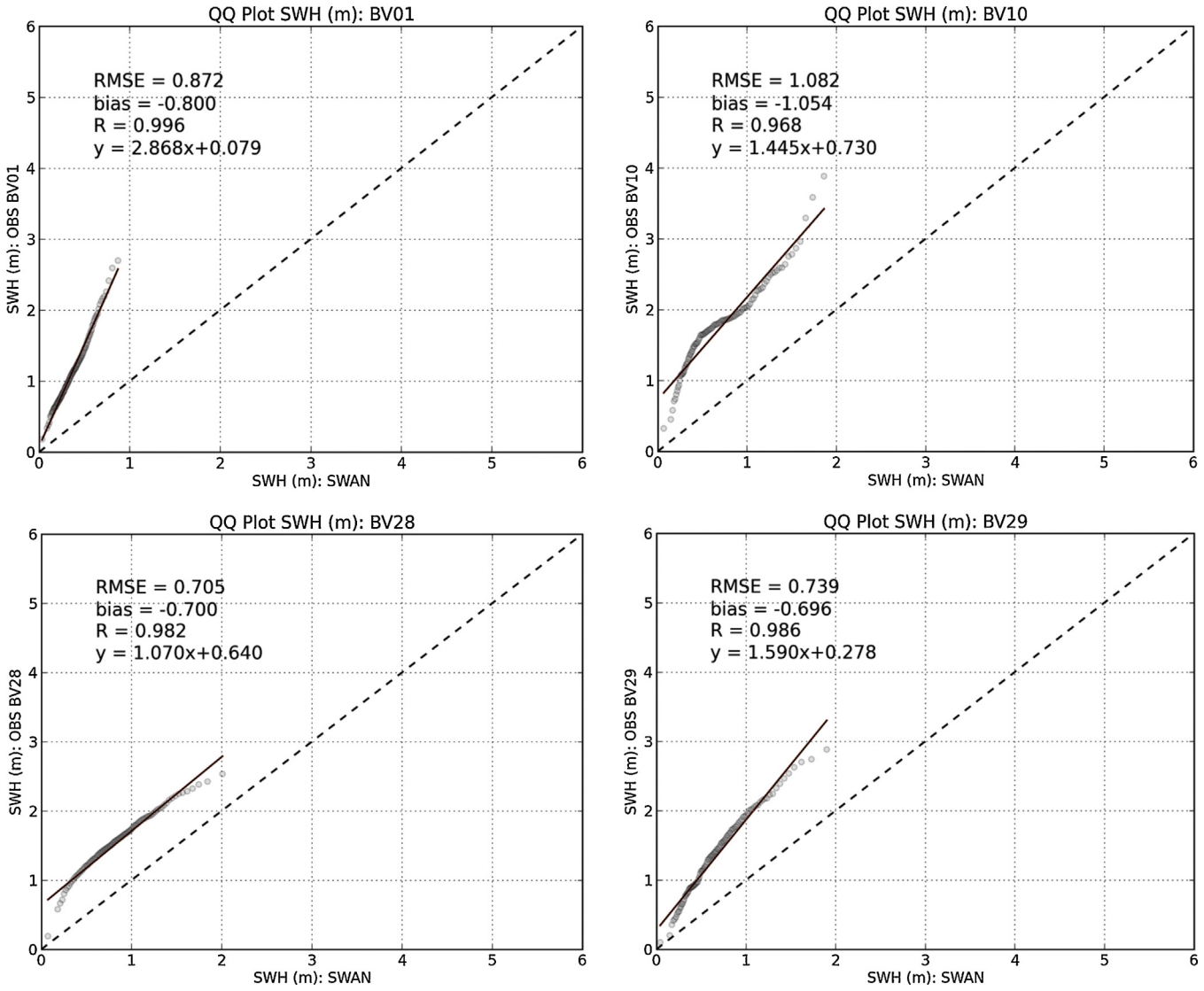

Fig. 3. Calibration carried out on mean wave field series. (Top left) VB1: Gulf of Uraba; (top right) VB10: Barranquilla; (bottom left) VB28: Guajira and (bottom right) VB29: San Andres.

Table 1
Location of the DIMAR buoys along the Colombian coast used for mean field validation.

Buoy	Coord [Deg]		Depth [m]	Available parameters	Record period
	Long West	Lat North			
Barranquila (41194)	−74°40′51″	11°09′41″	150	Hs,Tp,Dir	2008–2009
Pto. Bolivar (41193)	−72°13′02″	12°21′06″	150	Hs,Tp,Dir	2008–2010

Notations: Hs = Significant wave height, Tp = peak period, Dir = direction.

to 0.80 Hz with an $\sigma m + 1 = 1.1$ distribution and 36 directions (10 degree resolution). The time step employed was 900 s. The computational time was from 01/01/1979 00:00 UTC to 31/12/2011 21:00 UTC. The output time step was set to 3 h.

For the source terms, the best results were obtained for exponential growth due to wind and whitecapping dissipation using the WAM-Cycle 3 parameterization [26], non-linear wave–wave interactions by four components (Discrete Interaction Approximation, Hasselmann et al. [27]) and three components (Lumped Triad Approximation, Eldeberky [28]), depth-induced wave breaking (Battjes and Janssen [29]) and bottom friction (JONSWAP, Hasselmann et al. [30]). The SWAN model uses a phase-decoupled approximation based on the mild-slope equation to account for the refraction-diffraction processes [31].

As shown by Appendini et al. [4], the Caribbean areas are wind dominant due to the fact that the basin boundaries block distant swells. This is confirmed by Stopa et al. [3], who showed that enclosed basins like the Caribbean Sea are sheltered from distant swells and are dominated by wind waves produced locally. Lee et al. [32] showed that the parameterization of Komen et al. [26] performed well for wind seas, suggesting that the above parameterizations are a suitable approximation. The Komen et al. [26] parameterization has been tested for several authors for different climatic conditions with good results [33–35].

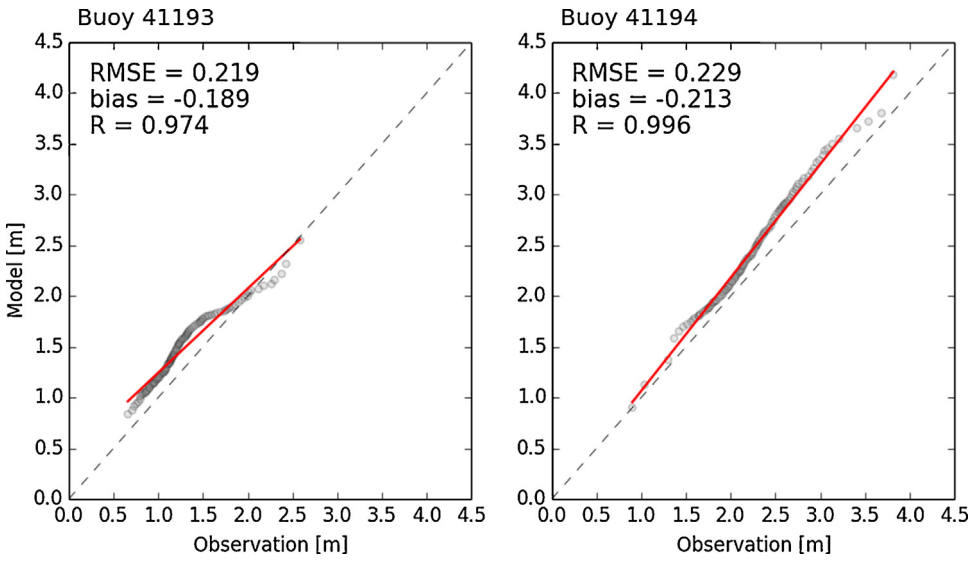

Fig. 4. Validation carried out on mean wave fields for significant wave height (Hs). (left) Puerto Bolivar – Buoy 41193; (right) Barranquilla – Buoy 41194.

Once the wave propagations were carried out, the results obtained by the SWAN model for significant wave height (Hs) were corrected in the probability domain with satellite data (Globewave). Fig. 3 shows the results for 4 virtual buoys located at strategic points along the Colombian Caribbean Coast (VB1: Gulf of Uraba; VB10: Barranquilla; VB28: Guajira and VB29: San Andres, see Fig. 1), where the high correlation ($R2$) for linear fit is clear. The linear fit coefficients, slope (m), intercept (b) and coefficient of determination ($R2$) were obtained for each virtual buoy. The parameters of the linear fit and equations obtained for each virtual buoy (VB) were employed as correction factors. The final results of the corrected mean fields were validated in the probability domain with the *in situ* buoys available from DIMAR (buoy 41194 and 41193, see Fig. 1 for location). Fig. 4 shows the results obtained, where the relatively small RMSE (RMSEPtoBolivar = 0.219 m and RMSEBarranquilla = 0.229 m) and high correlation measured by the root of the coefficient of determination R (RPtoBolivar = 0.974 and RBarranquilla = 0.996) verify that the mean wave fields are suitable to carry out blending with extreme wave fields.

3.2. Extreme wave field generation

Wave measurements from 2 oceanic buoys from the NOAA's National Data Buoy Center (NDBC) were employed (Table 2). Information for hurricane trajectories was obtained from the United States' Hurricane Research Division (HRD) and was used after being post-processed by UNYSIS (latitude, longitude, date, maximum sustained winds in knots and central pressure in the eye of the hurricane). The UNYSIS data available on http://weather.unisys.com/hurricane/provided the base information or hurricane modeling. This dataset has six hourly resolutions and covers a total of 33 years (1979–2011). For this period, complete and highly accurate information on central pressure and maximum sustained winds is available. Over the 33-year period, 47 hurricanes were selected; of which 8 correspond to category 5, 11 to category 4, 7 to category 3, 9 to category 2 and 12 to category 1. 33 tropical storms and 5 tropical depressions were also chosen. Bathymetry was obtained from the 2-min Gridded Global Elevation Dataset (ETOPO-1) available at: http://www.ngdc.noaa.gov/mgg/gdas/gd_desingnagrid.html#. Data was taken within the coordinates of 90°W and 58°W in longitude and 7°N and 23°N in latitude, and interpolated to a spatial resolution of 1/6°. The selection of the spatial resolution from the model and the other numerical parameters were taken from the methodology proposed by Montoya et al. [5].

The wind speed during hurricane conditions was obtained using the methodology proposed by Montoya et al. [5]. This methodology used the HURWIN asymmetrical hurricane model, based on the asymmetrical model by Collins et al. [36] and Jelesnianski [37] with improvements proposed by Lizano [38].

The aforementioned work was based on the hypothesis that hurricane models are able to adequately describe hurricane winds close to the eye and up to the radius of maximum winds (Rmax). In contrast, reanalysis databases do not adequately reproduce winds close to the hurricane eye but rather perform well in zones far away from it. Bearing this in mind, a methodology for the correction of hurricane winds is proposed using a combination of the winds from the parametric model HURWIN [38] and reanalysis data sources (in this case NARR).

The HURWIN model calculates wind velocities at a distance r from the hurricane eye based on certain constants and atmospheric variables like environmental pressure. This parametric wind model has been used previously with the SWAN model to generate extreme waves in the Colombian Caribbean [6,7] for specific hurricanes events.

Among the modeling considerations, forcings such as the mean surface currents and sea level variations were not included. As a preliminary step to obtain the historical series, calibration and sensitivity analyses were carried out of the different parameterizations so that the best modeling options could be defined (grids, time steps and the best parameterization to represent the physics of the phenomenon). This allowed the quality of the wind and wave model to be examined and limited the area of analysis to zones close to the hurricane eye where the principal shortcomings of the sources were assumed, as indicated by Montoya et al. [5].

To generate the extreme wave series, the WWIIITM multigrid version 3.14 third generation wave model [39,40] was employed. Montoya et al. [5], performed a comprehensive comparison between the WWIII models and the SWAN model during hurricane conditions employing ten (10) directional buoys in the Gulf of Mexico. They carried out a numerical simulation of the sea surface directional wave spectrum based on the quadrant location for the storm track and other wave parameters. They evaluated several parameterizations and their relationship with the drag coefficient. A number of conclusions were obtained for both models. Even for distant buoys, both models adequately reproduce the main

Table 2
Location of NOAA buoys in the Caribbean Sea employed for the calibration and validation of extreme events.

Buoy	Coord [Deg]		Depth [m]	Available parameters	Record period
	Long West	Lat North			
(42059)	−67°28′42″	15°11′00″	4802	Hs,Tp,Dir	2007–2013 Hourly
(42056)	−84°51′24″	19°48′06″	4684	Hs,Tp,Dir	2005–2013 Hourly

Notations: Hs = significant wave height, Tp = peak period, Dir = direction.

characteristics related to distance from the hurricane center and the quadrant location. The WWIII model performs best for buoys located in the right forward quadrant of the storm track, which generally has higher winds and greater significant wave height values. This indicates that the WWIII model gives a better spatial representation of wave parameters in the higher energy areas of the hurricane.

Regarding the best parameterization, comparisons were carried out between the available parameterizations in the multigrid version (3.14) of WWIII by Montoya et al. [5]. Comparisons were made between the Tolman and Chalikov [41] parameterization (referred to as TC) with and without limited drag (TCFLX3 and TCFLX2 respectively), the BAJ parameterization from Bidlot et al. [42], the WAM4 parameterization from Gunther et al. [43] and the ACC350 parameterization from Ardhuin et al. [44]. A much better performance for significant wave height can be seen for the TCFLX2 parameterization. However, based on the high sensitivity of these results to wind accuracy for the entire structure of the hurricane, a comprehensive calibration process is recommended.

Based on the little information available about capturing hurricane events and the results obtained by Montoya et al. [5], the WWIII model was selected to model extreme events in the Caribbean Sea. The following calibration process was developed for the Caribbean Sea employing the WWIII model. First, hurricane Dean from the year 2007 was selected for calibration, and Hurricane Emily from 2005 was chosen for validation. Next, a sensitivity analysis for all the options available in the 3.14 version for the Tolman and Chalikov [41] parameterization was performed. The results obtained for the Colombian Caribbean indicate better performance of the model with the Tolman and Chalikov [41] parameterization (TC), without the lineal growth from Cavaleri and Malanotte-Rizzoli [45] but with correction for the drag coefficient (C_D) for high winds [28]. The parameters were optimized using the Adaptive Random Search (ARS) method. Adaptive Random Search (ARS) is a tool [46] that can be used for obtaining regional optimal values using a search method. The object of the ARS is to find the optimal value of a model parameter; *i.e.*, a parameter value that exhibits the least error between the simulation run and the default run [47].

The parameters obtained in the calibration, validation and optimization process were employed for the modeling of all hurricanes in the Caribbean Sea. The parameter (STABSH) C_0 in the parameterization of TC96 minimizes the RMSE and corresponds to a value of 1.104. This parameter represents the effective wind speed proposed by Tolman [48] in response to problems related to: (i) the fact that when the model is tuned in a traditional way to obtain limited growth for stable conditions it underestimates deep-ocean wave growth, and (ii) effects of stability on the growth rate of waves, as identified by Kahma and Calkoen [49,50].

Fig. 5a shows the calibration results for Hurricane Dean (2007) for buoys 42056 and 42059 for the optimal value of C_0. Fig. 5b shows the validation for Hurricane Emily (2005), which occurred between August 13th 19:00:00 UTC and August 20th 12:00:00 UTC, for buoy 42056. The relatively small RMSE ($RMSE_{Dean}$ = 0.566 m for buoy 42059 and $RMSE_{Dean}$ = 0.663 m for buoy 42056) and high correlation measured by the coefficient of determination R^2 (R^2_{Dean} = 0.90 for buoy 42059 and R^2_{Dean} = 0.92 for buoy 42056) verifies that the

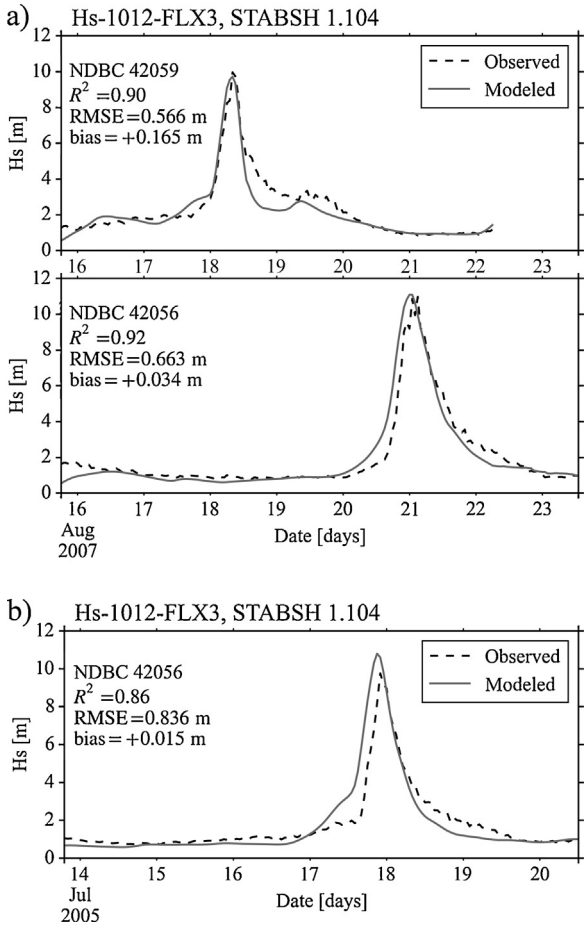

Fig. 5. (a) Observed and modeled significant wave height (Hs) for the optimal parameter C_0 obtained by the ARS method. The dashed line corresponds to buoy data while the solid line corresponds to modeled data. (b) Time series of significant wave height (Hs) for Hurricane Emily (2005) for buoy 42056 plotted against modeled values employing the calibrated parameters.

extreme wave fields are of a good enough quality to carry out the blending. These results are confirmed by the results obtained during the validation process for hurricane Emily (2005), with low values of $RMSE_{Emily}$ = 0.83 m.

With the parameters obtained during the calibration processes, all hurricanes selected were modeled employing the following settings for the WWIII model. The computational grid area extends from −90.0° to −58° in longitude and from 7.0° to 23.0° in latitude with a regular grid resolution of $\Delta x = \Delta y = 1/6°$. The numbers of nodes of the computational grid are 193 (x) and 97 (y). The spectral and directional resolution applied was 30 frequencies, varying from 0.042 Hz to 0.65 Hz with a $\sigma m + 1 = 1.1$ distribution and 36 directions (10 degree resolution). The time steps employed were 900, 900, 900 and 300 s for the global, spatial, intra-spectral and source term integration time steps respectively. The computational time was from 01/01/1979 00:00 UTC to 31/12/2011 21:00 UTC.

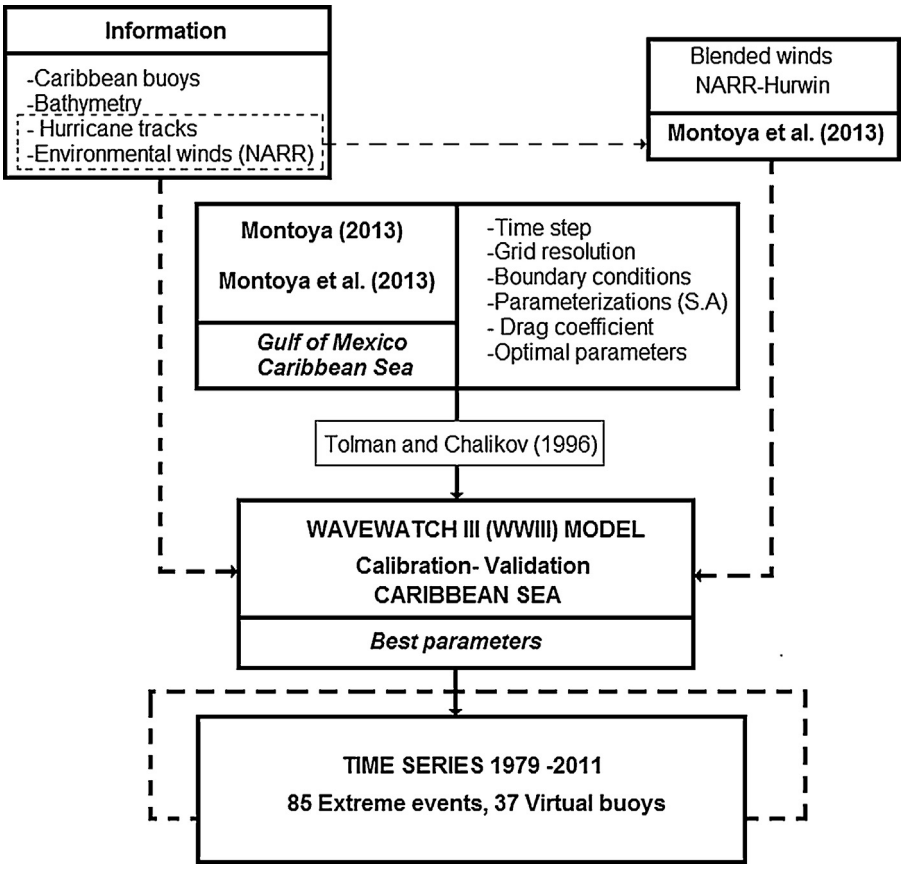

Fig. 6. Methodological diagram employed to generate extreme wave series in the Colombian Caribbean.

Fig. 6 summarizes the methodological process employed to generate extreme wave series using the parametric models.

3.3. Blending mean and extreme fields and datasheets

In order to merge the time series of average and extreme conditions, a simple physical approach was undertaken. Throughout the whole simulation time, when hurricanes have an influence on the wind environment for the Caribbean Sea, the blended wind speed for the whole space domain corresponds to the best performance. This implies that the time series of wave parameters for each virtual buoy obtained using the SWAN model could be replaced by the time series generated during extreme conditions using the WWIII model. To guaranty that the whole hurricane environment affecting the Caribbean Sea was replaced by the waves during a specific hurricane, the simulations were performed three days after and before the hurricane was reported by the Hurricane Research Division (HRD). The first twelve hours were eliminated to avoid numerical inconsistencies.

The information obtained is available with an hourly resolution from 1979 until 2011 for the most important wave variables, like significant wave height (Hs), peak period (Tp) and peak direction (Dir). The results of the methodology described above provide all of the wave information (Hs, Tp, direction) needed for the construction of histograms, probability and occurrence graphs (individual and combined), wave roses and conventional statistical parameters to describe the average and extreme behavior of the waves. The graphs and information generated by this type of methodology can be combined and presented together as guides or datasheets that allow a quick and simple visual analysis to be carried out of the wave behavior at a particular site (the results can be viewed at gis.invemar.org.co/erosioncostera/ or minas.medellin.unal.edu.co/gruposdeinvestigacion/oceanicos/virtualbuoys). The information obtained represents an important contribution to the development of coastal engineering and coastal management throughout the Colombian Caribbean. The basic design parameters can be acquired and a long-term analysis may be carried out from the historical series. To test the suitability of the generated time series for scientific and engineering applications, the next section describes a comprehensive analysis of the wave climate along insular and intercontinental areas of the Colombian Caribbean coast.

4. Wave climate analysis along the coast

The analysis of wave climate along the Colombian Caribbean coast was performed considering two important issues. The first is related to variations in the combined main wave parameters like significant wave height (Hs), peak period (Tp) and peak direction (Pdir). The second is related to the behavior of the significant wave height along the coast and its relationship with the ENSO phenomenon during the cold and warm phases (El Niño and La Niña).

4.1. Directional analysis along the coast

The directional analysis of waves along the Caribbean coast is a fundamental factor in the study of the different coastal processes and factors affecting the coast. It can also improve the information needed for the design of coastal structures. To analyze the directionality of the waves along the Colombian Caribbean coast, four (4) strategic sites were selected in the regions mentioned above. The chosen sites correspond to: (1) VB_5 for the area surrounding the Gulf of Morrosquillo, (2) VB_11 for Barranquilla, (3) VB_26 for

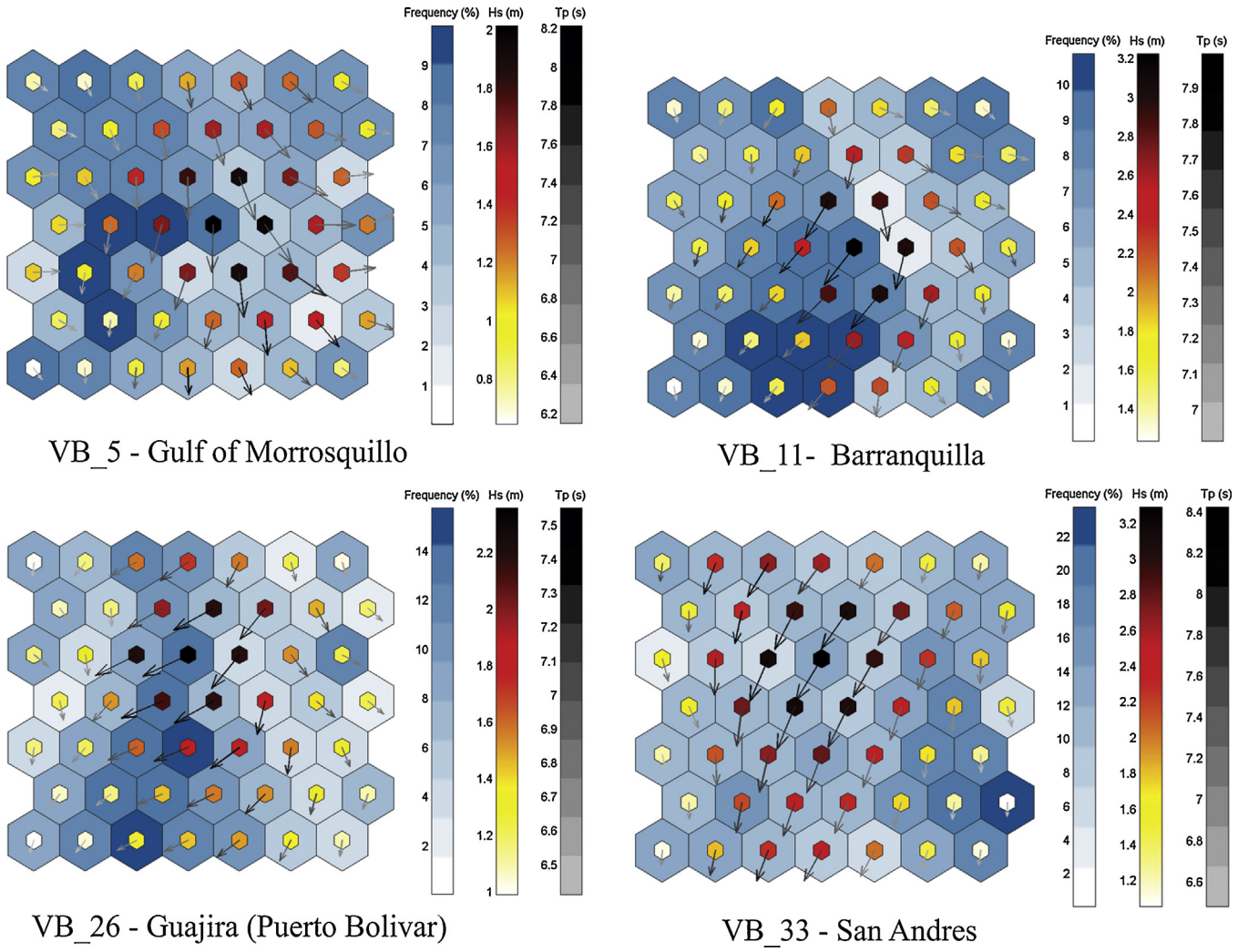

Fig. 7. Clustering techniques for some of the strategic virtual buoys in the Colombian Caribbean using the method proposed by Camus et al. [51].

the region of la Guajira in Puerto Bolivar, and (4) VB 33 for the most energetic region located toward the north of San Andres.

The Self Organizing Maps (SOM) clustering method proposed by Camus et al. [51] from the University of Cantabria allows for a simultaneous directional analysis of three of the following main wave variables: significant wave height (Hs), peak period (Tp) and predominant peak wave direction-Pdir (Pdir). This leads to the identification of the principal sea states, an easy visualization of the situation and a multidimensional probabilistic analysis. Fig. 7 shows the results obtained for each of the virtual buoys selected. In the figure, the smaller hexagon in a light yellow–dark red scale defines the Hs magnitude. The significant wave height (Hs), the peak period (Tp) and the predominant peak wave direction-Pdir (Pdir) are represented by the size, the intensity of the gray color, and the direction of the arrow, respectively [51]. The color of the outer hexagon filled in shades of blue represents the relative frequency of (Hs). The gray scale on the arrows demonstrates the magnitude of the period employed (in this case peak period Tp). The maximum and minimum values represent the maximum and minimum magnitudes of the variables Hs and Tp obtained during classification. This technique is capable of detecting all the possible sea states and similar clusters are located together in the projection space. The magnitudes of the parameters which define the centroids vary smoothly from one cell to another [51].

It is important to mention that clustering techniques only give the most representative data. In particular, the SOM method tends not to classify the most extreme values very well, unlike methods such as the K-means Algorithm (KMA) and the Maximum Dissimilarity Algorithm (MDA). For an adequate interpretation of the results, the different groups obtained during classification were put into the SOM graph using the following terminology: The specific hexagon (cluster) $S(i,j)$ represents the wave parameters for a given sea state, with i as the column and j as the row position on the lattice (7×7 for this research). The directional analysis for each region, represented by a corresponding virtual buoy (VB), is shown in the following section. For the analysis of wave direction, waves were measured from the north in a clockwise direction and toward the direction shown by the arrow.

4.1.1. Gulf of Morrosquillo virtual buoy (VB_5)

The results show that the most frequent sea states go from a north-easterly and northerly direction toward the southwest and south respectively. The four most frequent sea states show a high variability and low Hs values of around 0.5 m through to 1.0, 1.3 and 1.7 m. Occurrence frequencies are around 9%, representing about 35% of the complete data ($S(2,4)$, $S(3,4)$, $S(2,5)$ and $S(2,6)$). The most energetic sea states with low occurrence frequencies of around 3% to 5% travel toward the south and southeast (varying from approximately 160° to 180°) ($S(5,3)$, $S(5,4)$, $S(5,5)$ and $S(4,4)$).

For this area the highest peak periods are observed toward the southeast. Further northeast, the virtual buoy in the Gulf of Morrosquillo shows clockwise components toward the southwest in

accordance with the behavior of wind direction along the coastal areas of the Caribbean Sea. However, waves in a south-easterly direction may be generated in periods in which the trade winds from the Pacific enter the Caribbean and change direction due to the presence of local winds coming from the southeast, or, more likely, due to counter clockwise variations in the wind. For VB_5 the highest values of peak direction are observed slightly toward the southeast, with two important components (S(5,5) and S(5,6)) and average Hs values of around 2 m and 1.5 m respectively and a peak period of around 8 s. The sea state S(5,5) represents the most energetic component (highest significant wave height and peak period) and has an occurrence frequency of around 4%. Such behavior is consistent with the results observed for wind speed variability in this region. Furthermore, it confirms the strong relationship between the wind speed and ocean waves in the Caribbean Sea presented by Stopa et al. [3], who shows that ocean swells from distant areas in the Atlantic are blocked.

4.1.2. Barranquilla virtual buoy (VB_11)

The Barranquilla virtual buoy shows that the most energetic ocean waves in the Colombian Caribbean Sea come from the northeast (approximately 210°), with average values of around 3.2 m and an occurrence frequency of around 8% (S(4,4)). The maximum occurrence frequency sea states with an individual frequency of about 10% appear to come from a north-easterly to south-westerly direction, with average significant wave heights of 1.5, 1.6, 1.8, 2.3 and 2.5 m. These components are found predominantly in the Barranquilla region and are further southwest than the more energetic and frequent components of the virtual buoys in the Gulf of Morrosquillo, the Gulf of Uraba and even in Cartagena. As discussed above, this behavior is associated with the counter clockwise gyre of trade winds from the northeast along the Colombian Caribbean coast. The mean values of significant wave height are around 1.8 m (observed for several sea states) and have a high variability, with directions varying from 90° toward the east to 220° toward the west.

Similarly, some sea states exist with very low significant wave heights (Hs) and directions between 140° and 210° (south-easterly and south-westerly). These sea states are S(7,1), S(1,1), S(1,6), S(1,7), S(2,7), S(7,7) and S(7,6). High peak period values of approximately 8 s were obtained for the predominant and most energetic sea states (S(4,4) and S(4,3)) which were toward the southwest.

4.1.3. La Guajira virtual buoy (VB_26)

The Guajira buoy demonstrates a slight decrease in the maximum wave magnitude, with a value of approximately 2.4 m for the most energetic sea state (S(4,3)). The most frequent and energetic sea states mentioned above are again predominantly in a southwesterly direction, but slightly more toward the south compared to the results obtained for the Santa Marta region (250° approximately). The most frequent cases show values of significant wave height of about 1.3 m and 1.8 m, average periods of 6.5 s and 7 s, and occurrence frequencies of about 13% and 14% (S(3,7)). The greatest wave heights appear with a slightly lower frequency than the buoys located toward the west of the Colombian Caribbean Sea, and have periods of around 7.5 s.

The least frequent sea states in the data were given for significant wave heights varying from 1.0 to 1.7 m and directions with more variability than the most energetic waves. Directions vary from 135° (east to west) to a slightly south-westerly direction of around 210°. Periods are from 6.5 s to a maximum of 7 s. The lowest sea state values for the Guajira buoy vary between 170° toward the southeast and 190° toward the southwest. Average significant wave height values are around 1.0 m and peak periods are 6.0 s.

4.1.4. San Andres Virtual buoy (VB_33)

The most important insular region in the Colombian Caribbean Sea is around the islands of San Andres and Providence. Both islands are located near the western zone of the political division of the Colombian Caribbean Sea, where the northeast trade winds provide the main forcing. The results show a predominant south-westerly direction for most sea states in the SOM graph. The most energetic waves present average significant wave height values of around 3.2, and peak periods of 8.2 s toward the southwest (210° approximately) (S(4,2), S(4,3), S(3,3), S(3,4) and S(4,4)).

The peak period for the full time series for the virtual buoy in the eastern zone of the island of San Andres varies between 6.2 and 8.4 s, with the highest values in a south-westward direction (in the same direction as the highest significant wave height values). When light winds occur in the Caribbean Sea (March, April, May, September and October) and the ocean waves have low energy and low significant wave height values, an important southward and slightly south-eastward variation in wave direction is observed. The significant wave height varies from 1.0 to 1.6 for these sea states and the peak period varies from about 6.2 s to 7 s.

4.1.5. General wave pattern

General observation of the graphs clearly shows how the orders of magnitude of the more energetic waves are lower in the westerly direction toward the Gulf of Uraba. Here values vary between approximately 0.7 and 2.2 m for Hs and range from around 6.4 to 8.2 s for peak period (Tp). Significant wave height (Hs) increases eastward. The greatest values occur in Barranquilla, reaching a maximum of 3.2 m. Toward the north in the direction of La Guajira, the average magnitudes of significant wave height slightly decrease to values of around 2.4 m. The lowest maximum values for peak period (around 7.5 s) are found in this region.

In general, the most energetic waves, which are generated by trade winds, come from the northeast. However, in the Guajira region there is a gradual change in predominant wave direction toward the west. Also, in the Gulf of Morrosquillo and toward the west of the Caribbean Sea, the waves show a northerly and northwesterly direction. The mean local wind circulation patterns along the Caribbean coast show very similar behavior, with predominant directions to the west or slightly southwest in the region of la Guajira and gradual variations that are more southerly toward the Gulf of Morrosquillo. These results indicate a greater influence of local wind (stronger) on wave patterns in the Colombian Caribbean Sea, especially near Barranquilla where the mean wind circulation patterns show a zone of strong winds.

The spatial variability along the Colombian Caribbean coast based on the SOM analysis shows that the highest directional variability occurs on the west coast near the Gulf of Morrosquillo. This variability decreases toward the most energetic areas located near Barranquilla and strongly decreases for the insular zones of San Andres.

4.2. Influence of hurricanes and macroclimatic phenomena in the wave climate

It was identified that the behavior of waves along the continental Colombian Caribbean coast differs considerably depending on geographic location and meteorological conditions (Displacement of the Intertropical Convergence Zone (ITCZ) through the Caribbean Sea and the Hurricane Season, among others). To test this hypothesis, in the same graph for each virtual buoy (from VB1 to VB37, numbered on the x axis), Fig. 8 presents the maximum wave height observed during hurricane conditions, the maximum significant wave height during mean wave fields (without hurricanes), and the average significant wave height for the full time series. The results showed that the influence of tropical storms and hurricanes whose

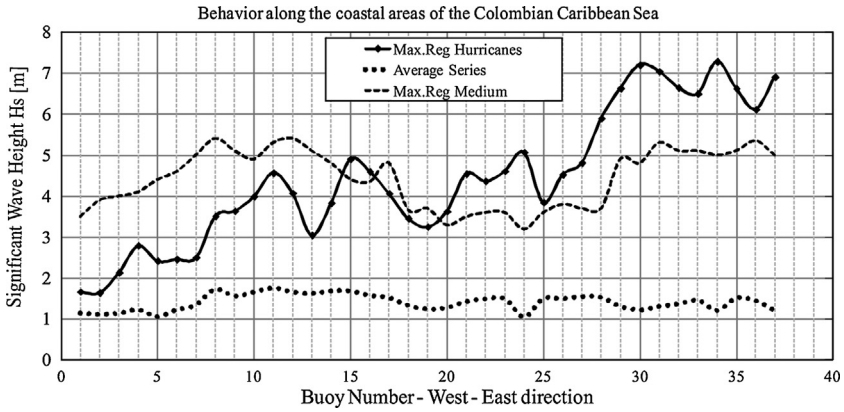

Fig. 8. Comparison of wave fields (mean and extreme) along the continental Colombian Caribbean coast.

trajectories pass close to Colombian Caribbean coast doesn't affect the whole coastline in the same way. From the virtual buoy located near the Gulf of Uraba (VB01) to approximately Buoy 13 near Barranquilla (see Fig. 1), the mean values exceed the wave heights estimated for extreme events. This behavior is easily explained by the fact that their positions are relatively further away from the most likely track areas.

Furthermore, during the passage of hurricanes these zones experience a substantial reduction in wind speed due to a decrease in the pressure gradients and alterations in the pressure environment. This wind speed and pressure relationship influences the local wind waves and produces a reduction in the associated energy. At the same time, the strong wave components located near the hurricane eye demonstrate a sharp decrease in wave energy. Another important aspect is related to the energy in the four quadrants present during hurricane translation, as was observed by authors such as Young [52], Zhuo et al. [53], Moon et al. [54] and Montoya et al. [5]. The results show that the most energetic waves are located in the right forward quadrant of hurricane translation. This means that for the Caribbean Sea, where the most frequent hurricanes travel from east to west, the more energetic areas are located toward the north in the direction of the Greater Antilles (Cuba, Haiti and Puerto Rico).

Toward the north of the Colombian Caribbean Sea around the Guajira region, most hurricanes pass close to land, and as a result more energetic waves are produced. From VB20 to VB28 (see Fig. 1), in the most critical cases the wave height projections for extreme fields exceed the values of the mean series by up to two times. When comparing the maximum values obtained during average conditions (without hurricanes) and the maximum values obtained during hurricane occurrence, hurricanes are clearly the cause of the most energetic waves in the north of the Colombian Caribbean Sea. This is due to the close distance of the area to the hurricane track, and therefore, the most intense winds. It is possible to note that the behavior of both series of maximum waves for each location follows a similar tendency with respect to their peaks and troughs. This reinforces previously accepted knowledge about the direct dependency that exists between wind (both extreme and average) and wave phenomena.

The coastal areas from virtual buoys 16 to 20 (close to Santa Marta) present very similar behavior for both values, showing a smaller influence of hurricane activity (decreasing south-westward and increasing north-eastward).

For the San Andres and Providencia islands (VBs 29 to 37 in Fig. 8, see Fig. 1), the results for extreme values show an important increase in the energy associated with both conditions (extreme and average) when compared with most of the continental areas of the Colombian Caribbean Sea (VBs 1 to 27 in Fig. 8). For the maximum average (Max.Reg Medium), Fig. 8 shows values of around 5 m for all the VBs located around this insular area. Very similar results were obtained by the virtual buoys located near Barranquilla, Cartagena and Santa Marta (Fig. 1) in the continental zone. It should be noted that these are Colombia's most significant regions for tourism (insular and continental) and commerce (continental) in the Caribbean Sea.

For the Maximum values associated with hurricane activity, Fig. 8 shows more critical conditions after an abrupt change around virtual buoy 25 located in the Guajira region. Significant wave height reaches maximum values of around 7 m for the insular zones (VBs 29 to 37) and values varying from 4.5 m to 5.8 m for VBs 26, 27 and 28 in the Guajira region. These results are consistent with those obtained by Montoya [25] who showed that the Guajira region and the insular zones of San Andres and Providencia were the most energetic areas during hurricane activity. The minimum values associated with hurricane activity (around 2 m) occur toward the south near the Gulf of Uraba and the Gulf of Morrosquillo.

These types of comparisons are of vital importance for engineering and coastal management, especially for public and private entities responsible for making decisions in coastal cities. It can be clearly and simply established which regions require special attention due to the effects of the phenomena associated with waves, such as erosion, storms and floods, among others. Despite the fact that the data obtained from the numerical modeling has been calibrated and validated, it should be taken into account that these values are only a reference for wave magnitude in deep waters near the coast. Therefore, any future coastal projects must first include an adequate coastal study to verify this data.

To complete the analysis of wave climate along the coastal areas of the Colombian Caribbean Sea (insular and continental), and to study the effect of the influence of the ENSO phenomena's warm and cold phases, Fig. 9 shows the annual cycle for the same buoys employed during the clustering analysis.

As has been observed by authors such as Wang [55], Ruiz and Bernal [15], Stopa et al. [3], Montoya [25] and Montoya and Osorio [2], the ENSO and other macroclimatic phenomena such as the North Atlantic Oscillation (NAO) affect the climatology of tropical areas like the Caribbean Sea. Such phenomena strongly affect wind speed patterns and wind waves. The aforementioned authors have researched the general patterns of wind speed during both phases of the ENSO phenomenon, but few have investigated its influence along the Colombian coast and the direct impact on wave climate behavior.

The results for the general patterns show four main seasons in the annual cycle with two maximum values. The highest values during the year coincide with the highest values of synoptic wind (or trade wind). The first maximum is during the months of December–January–February (DJF). The second is during the months of June–July–August (JJA), again showing a significant

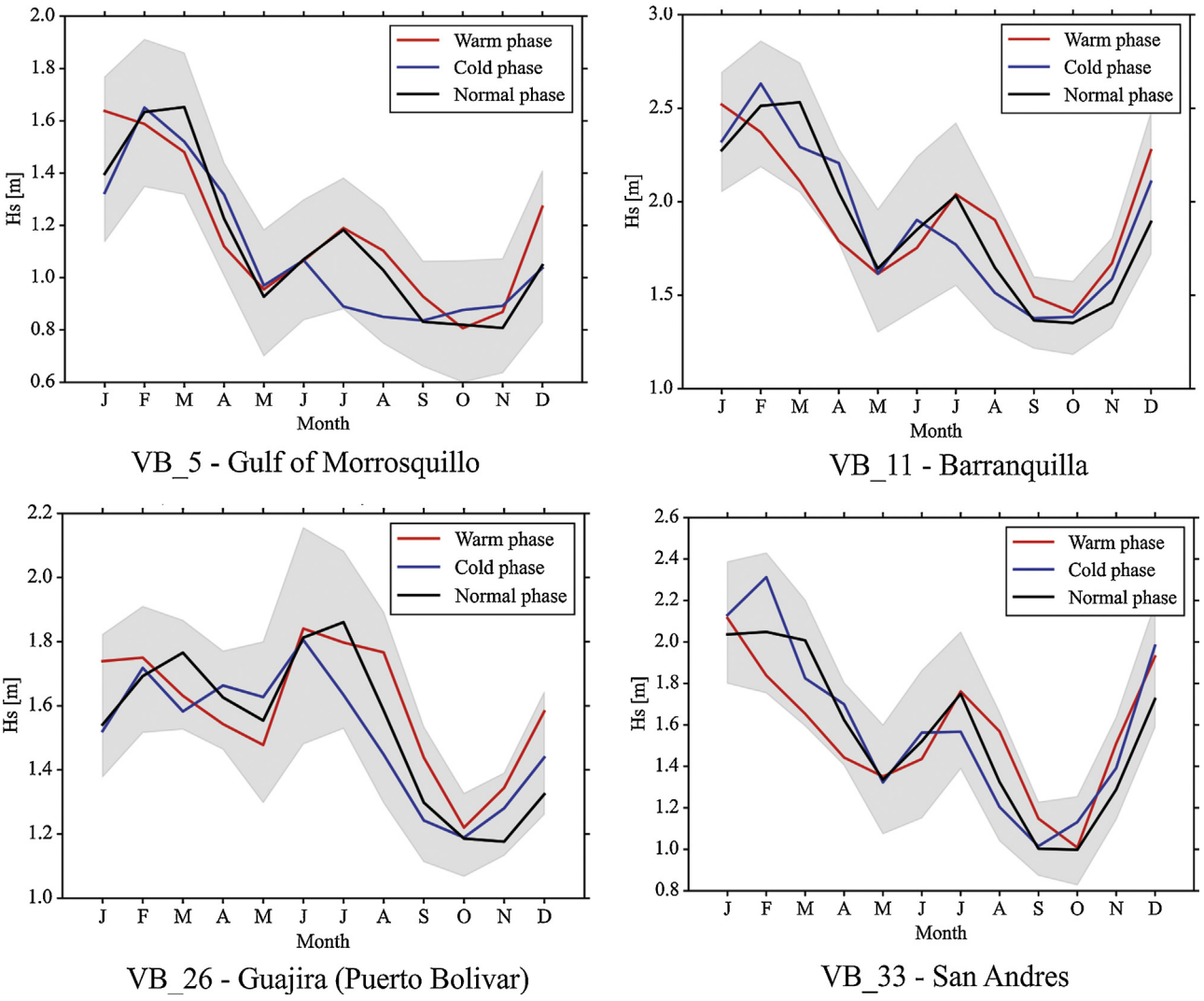

Fig. 9. Annual cycle along the continental and insular areas of the Colombian Caribbean coast and its relationship with both phases of the ENSO macroclimatic phenomenon (El Niño, La Niña). The gray band represents the variability of all years of the study period.

increase in the values of significant wave height. The first minimum value is during the months of March–April–May (MAM) and the second is during the months of September–October–November (SON), with further weakening of the trade winds from the northeast. Authors like Mesa et al. [14] and Ruiz [56], among others, showed that the climatology in the majority of the Caribbean Sea can be divided into these four main trimesters. This behavior is observed for most of the virtual buoys and during both phases of the ENSO (the cold phase – La Niña, and the warm phase – El Niño) even during normal seasons.

A deeper analysis comparing the warm and cold phases shows several important points. During the seasons (DJF) and (MAM), the cold phase of the ENSO (La Niña) presents higher values than during the warm phase (El Niño) for the same climatic periods. This is due to the intensification of the trade winds in the Caribbean Sea. However, this situation is reversed during the warm phase around July in the third season of the year (JJA). These results confirm those observed by Ruiz and Bernal [15] and Ruiz [56], who show contrary behavior for wind speed during the Niña and Niño phases in the wet and dry seasons at several sites in the Caribbean Sea. The results observed confirm the fact that despite the spatial variability of these patterns throughout the main region of the Caribbean Sea, similar results are observed along the Colombian Caribbean coast.

An analysis of the most and least energetic months during the four seasons reveals several important variations along the coast. The most energetic months were observed around February for the majority of the buoys, with the exception of one virtual buoy located toward the north in the Guajira Region (VB 26) which showed its highest value during July. These results were verified for all the buoys located near La Guajira, starting with virtual buoy 23 in the middle of the region (see Fig. 1), and for both the cold and warm phases of ENSO (results not shown here). These results suggest minor changes between the two seasons (DJF and JJA) and a smaller influence of the Caribbean Low Level Jet (LLJ), which has also been reported by the aforementioned authors for this region.

For low energy conditions during the seasons of (MAM) and (SON), the latter season presents the lowest values of significant wave height of all the virtual buoys selected for this research (insular and continental). The lowest values oscillate between September (S), October (O) and even November (N). A strong change exists between the higher energy season (MAM) and the lower energy season (SON) for all the insular and continental areas of the Colombian Caribbean coast.

A full analysis of the annual cycle along the coast confirms that the more energetic areas are around the Cartagena, Barranquilla and Santa Marta, where a region of strong winds is observed

(values below 2.5 m in most cases). The significant wave height decreases toward the southwest around the Uraba region, and slightly decreases toward the Guajira in the northeast. For the insular zones of San Andres and Providencia, slightly higher values are observed when compared with the areas mentioned above. This confirms that the insular zones of Colombia are the regions most exposed to ocean wave damage (erosion and flooding, among other problems) for average and extreme conditions during hurricane occurrence.

5. Discussion and conclusions

The proposed methodology allows different techniques and statistical tools to be combined for the calibration and validation of models in order to obtain historical series (gis.invemar.org.co/erosioncostera/ or minas.medellin.unal.edu.co/gruposdeinvestigacion/oceanicos/virtualbuoys) in the Caribbean Sea for insular and continental areas. These series are free and reliable and are an essential tool for the development of coastal projects in Colombia. This methodology aims to fill some of the gaps described by previous authors [3,4,57–60]. These gaps are related with the low spatial and temporal resolution of wind reanalysis datasets used for long-term wave hindcasting to describe cyclonic events in tropical regions.

Appendini et al. [57] reports that the highest mean significant wave height, found off the coasts of Colombia and Venezuela, corresponds to the waves generated by the CLLJ (Caribbean low-level jet), as described by Wang [55]. The work presented here highlights and confirms these results, but at the same time goes into more depth concerning the different seasons in the Colombian Caribbean. It is possible to identify a climate that is generally controlled by the behavior of trade winds from the northeast, with the occurrence of hurricane events in the second semester of the year. Extreme phenomena like hurricanes are governed by alterations in the temperature of the sea surface and atmospheric pressure that are generally not adequately captured by reanalysis databases. Therefore, the simple and robust methodology presented here allows the modeling of extreme events and average conditions to be combined independently and at the same time considers the physics of both statistical families.

During average conditions, the most energetic waves in the continental Colombian Caribbean were found in the regions of Cartagena, Barranquilla and Santa Marta. San Andres and Providence had the most energetic waves of the insular areas, where stronger trade winds from the northeast generate local sea waves. Such waves have a predominant south-westerly direction and the greatest occurrence frequencies. This local hindcast confirms the global hindcasts presented by other authors [3,60,61]. The maximum values associated with average conditions (mainly associated to cold fronts) show that ocean wave energy in the coastal areas of the Caribbean Sea (VBs 1 to 28) decreases southward and slightly toward the North. However, during extreme conditions (associated to hurricanes) the strong influence around the region of La Guajira and the insular zones of San Andres and Providencia is quite evident when compared with other regions along the coast (Fig. 8).

The new approach presented in this study suggests a dipole between the north-east (hurricane influence) and south-west (cold fronts) in extreme events that has not been reported before. This work confirms what has been reported in previous studies where significant wave height can be magnified by the waves generated by the passage of polar fronts [19] during the first three months of the year and the passage of storms and hurricanes between June and November [7]. Furthermore, our analysis of extreme events during hurricane conditions along the Colombian Caribbean coast shows how the evolution of more energetic waves increases with a positive trend from the southwest (Uraba Gulf) to the northeast (Guajira). In the south-western regions, the low energy values are associated with the long distance to the eye of the most frequent hurricanes, the low speed of local winds and infrequent low energy hurricanes passing nearby. In the north-eastern region, there are high significant wave height values associated to short distances to the eye of the hurricanes where more energetic waves and winds are expected.

During the ENSO conditions, the influence of La Niña and El Niño is opposite for most of the buoys. Enfield and Mayer [62] report that tropical Atlantic sea-surface temperature variability is correlated with Pacific ENSO variability in several regions. In El Niño this occurs as a result of reductions in the north–east trade wind speed at the surface. However, we found that this hypothesis is only valid during the final seasons of the year (DJF) and during (MAM), where the highest values of wave height occur during the cold phase (La Niña) and low values occur during the warm phase (El Niño). During the (JJA) season, this situation is reversed, with the highest values occurring during El Niño and low values appearing during La Niña. Therefore, additional information has been found for the Caribbean region that is not evident in previous work with a more global focus [3,43]. Previous work showed that La Niña had a greater influence on North Atlantic regions affected by trade winds blowing from West Africa to the Caribbean.

The seasonal variability between the 4 climatic periods reported previously [31,61] is confirmed in this study. The most energetic ocean waves are observed during the (DJF) season for both the warm and cold phases of the ENSO, showing large differences compared with the (JJA) season for most of the virtual buoys. However, the majority of the Guajira region has very similar values of wave height for both the (DJF) and (JJA) seasons and both phases of the ENSO, proving that this region has less variability over one year. However, VB26 (Fig. 9) presents a small increase in wave height during July (for all ENSO phases). These results can be associated with the less influence of the North Atlantic high pressure area (NAO) on the climatology of the eastern part of Colombia. There is a minor change between the (DJF) and (JJA) seasons and a lesser influence of the Caribbean Low Level Jet (CLLJ). This kind of relationship was not clear in previous studies that were more global [3,61].

Acknowledgements

This research was carried out thanks to the cooperation of the Oceanic Studies Group (*Grupo Oceánicos*) from the *Universidad Nacional* of Colombia, GICI and GICAMH from the *Universidad de Medellin* and the *Geosciences Area of the Physics Department from the Universidad del Norte*. Gratitude is given to the Institute of Marine and Coastal Investigation (*Instituto de Investigaciones Marinas y Costeras, INVEMAR*) *José Benito Vives De Andréis*, and the National Coastal Erosion Program financed by COLCIENCIAS with special cooperation from agreement number 153. The authors would like to acknowledge the support of Paula Camus et al., Fernando Mendez and the climatic group from IH Cantabria for developing the SOM methodology employed in this paper for directional analysis. Furthermore, the authors would like to thank DIMAR (from the Colombian Navy) and the NOAA for making the buoy data used for the validation of this methodology available. The authors would also like to thank Santiago Ortega and Natalia Moreno for their initial contribution to the modeling and data analysis.

References

[1] Ortega S, Osorio AF, Agudelo P. Estimation of the wave power resource in the Caribbean Sea in areas with scarce instrumentation. Case study: Isla Fuerte, Colombia. Renew Energy 2013;57:240–8.
[2] Montoya RD, Osorio AF. Methodology to correct wind speed during average wind conditions: application to the Caribbean Sea. J Atmos Oceanic Technol 2014;31:1922–45.
[3] Stopa JE, Cheung KF, Tolman HL, Chawla A. Patterns and cycles in the Climate Forecast System Reanalysis wind and wave data. Ocean Modell 2013;70:207–20.
[4] Appendini CM, Torres-Freyermuth A, Oropeza F, Salles P, López J, Mendoza ET. Wave modeling performance in the Gulf of Mexico and Western Caribbean: wind reanalyses assessment. Appl Ocean Res 2012;39:20–30, http://dx.doi.org/10.1016/j.apor.2012.09.004.
[5] Montoya RD, Osorio AF, Ortiz-Royero, Ocampo-Torres FJ. A wave parameters and directional spectrum analysis for extreme winds. Ocean Eng 2013;67:100–18.
[6] Ortiz JC, López F, Estrada E, Bacca L. Study and simulation of Hurricane Joan on Colombian Caribbean coast including Isla de San Andrés in 1988. Rev Colomb Soc Phys 2008;40(2) [in Spanish].
[7] Ortiz JC. Exposure of the Colombian Caribbean Coast, including San Andrés Island, to Tropical Storms and Hurricanes, 1900–2010. Natural Hazard J (2012) 2012;61, 815-827 R.
[8] Swail VR, Cox AT. On the use of NCEP-NCAR reanalysis surface marine wind fields for a longterm North Atlantic wave hindcast. J Atmos Oceanic Technol 2000;17:532–45.
[9] Lionello P, Cogo S, Galati MB, Sanna A. The Mediterranean surface wave climate inferred from future scenario simulations. Global Planet Change 2008;63:152–62.
[10] Pilar P, Guedes Soares C, Carretero JC. 44-year wave hindcast for the North East Atlantic European coast. Coast Eng 2008;55:861–71.
[11] Cieślikiewicz W, Paplińska-Swerpe B. A 44-year hindcast of wind wavefields over the Baltic Sea. Coast Eng 2008;55:894–905.
[12] Dodet G, Bertin X, Taborda R. Wave climate variability in the North-East Atlantic Ocean over the last six decades. Ocean Model 2010;31(3–4):120–31.
[13] Reguero BG, Menéndez M, Méndez FJ, Mínguez R, Losada J. A Global Ocean Wave (GOW) calibrated reanalysis from 1948 onwards. Coast Eng 2012;65:38–55.
[14] Mesa O, Poveda G, Carvajal L. Introduction to the climate of Colombia. 1st Ed Medellin: National University of Colombia; 1997, 390 p. [in Spanish].
[15] Ruiz-Ochoa M, Bernal G. Seasonal and interannual variability of the wind in the NCEP reanalysis data/NCAR in Colombia Basin, Caribbean Sea. Adv Water Resour 2009;20:7–20 [in Spanish].
[16] Maza M, Voulgaris G, Subrahmanyam B. Subtidal inner shelf currents off Cartagena de Indias, Caribbean coast of Colombia. Geophys Res Lett 2006;33(L21606):1–5.
[17] Goldenberg SB, Landsea CW, Mestas-Nuñez AM, Gray WM. The recent increase in Atlantic hurricane activity: causes and implications. Science 2001;293:474–9.
[18] Taylor MA, Alfaro EJ. Climate of Central America and the Caribbean. Encyclopedia of world climatology. Encycl Earth Sci Ser 2005:183–9.
[19] Ortiz JC, Otero LJ, Restrepo JC, Ruiz J, Cadena M. Cold fronts in the Colombian Caribbean Sea and their relationship to extreme wave events. Nat Hazards Earth Syst Sci 2013;13:2797–804, http://dx.doi.org/10.5194/nhess-13-2797-2013.
[20] Mesinger F, DiMego G, Kalnay E, Mitchell K, Shafran PC, Ebisuzaki W. North American regional reanalysis. Bull Am Meteorol Soc 2006;87:343–60.
[21] Amante C, Eakins W. ETOPO1 1 Arc Minute Global Relief Model. Procedures, Data Sources and Analysis. NOAA Technical Memorandum NESDIS NGDC-24; 2009.
[22] Booij N, Ris RC, Holthuijsen LH. A third generation wave model for coastal regions. J Geophys Res 1999;104(C4):7649–66.
[23] SWAN-team. SWAN Cycle III version 40.85. Scientific and technical documentation; 2011.
[24] Moeini MH, Etemad-Shahidi A. Application of two numerical models for wave hindcasting in Lake Erie. Appl Ocean Res 2007;29:137–45.
[25] Montoya RD [Ph.D. thesis] Study of the interactions between large scale climate phenomena and waves in the Caribbean Sea: methodologies to correct wind speed during average and hurricane conditions for wave climate analysis. Univerisidad Nacional de Colombia; 2013, 340 pp.
[26] Komen GJ, Hasselmann S, Hasselmann K. On the existence of a fully developed wind-sea spectrum. J Phys Oceanogr 1984;14:1271–85.
[27] Hasselmann S, Hasselmann K, Allender JH, Barnett TP. Computations and parameterizations of the nonlinear energy transfer in a gravity-wave spectrum. Part II: Parameterizations of the nonlinear energy transfer for application in wave models. J Phys Oceanogr 1985;15:1378–91.
[28] Eldeberky [Ph.D. dissertation] Nonlinear transformation of wave spectra in the nearshore zone. The Netherlands: Delft University of Technology, Department of Civil Engineering; 1996.
[29] Battjes JA, Janssen JPFM. Energy loss and set-up due to breaking of random wave. In: Proc 16th Int Conf Coastal Engineering. 1978. p. 569–87.
[30] Hasselmann K, Barnett TP, Bouws E, Carlson H, Cartwright DE, Enke K, et al. Measurements of wind-wave growth and swell decay during the JointNorth SeaWave Project (JONSWAP). Ergaenzungsheft zur Deutschen Hydrographischen Zeitschrift, Reihe A 1973;(8):12–95.
[31] Holthuijsen LH, Herman A, Booij N. Phase-decoupled refraction-diffraction for spectral wave models. Coast Eng 2003;49:291–305.
[32] Lee HS. Evaluation of WAVEWATCH III performance with wind input and dissipation source terms using wave buoy measurements for October 2006 along the east Korean coast in the East Sea. Ocean Eng 2015;100:67–82.
[33] Lv X, Yuan D, Ma X, Tao J. Wave characteristics analysis in Bohai Sea based on ECMWF. Ocean Eng 2014;91:159–71.
[34] Akpınar A, van Vledder GP, Ihsan Kömürcü M, Özger M. Evaluation of the numerical wave model (SWAN) for wave simulation in the Black Sea. Conti Shelf Res 2012;50–51:80–99.
[35] Guillou N. Evaluation of wave energy potential in the Sea of Iroise with two spectral models. Ocean Eng 2015;106:141–51.
[36] Viehnaman CJ. A simplified empirical model for hurricane wind fields. In: Paper No. otc 1346, Offshore Technology Conference. 1971.
[37] Jelesnianski C. SPLASH (Special program to list amplitudes of surges from hurricanes); Part II: General tracks and variant storm condition. NOAA, Tech, Memo.; 1974. NWS TDL-52, Silver Spring.
[38] Lizano O. Wind model fit to a wave generation model for forecasting during hurricanes. Geophysics 1990;33:75–103 [in Spanish].
[39] Tolman HL. User manual and system documentation of WAVEWATCH-III version 2.22. NOAA/NWS/NCEP/MMAB; 2002.
[40] Tolman HL. User manual and system documentation of WAVEWATCH III version 3.14. NOAA/NWS/NCEP/MMAB Technical Note 276; 2009, 194 pp.
[41] Tolman HL, Chalikov D. Source terms in a third-generation wind-wave model. J Phys Oceanogr 1996;26:2497–518.
[42] Bidlot JR, Abdalla S, Janssen PA. A revised formulation for ocean wave dissipation in CY25R1. Tech. Rep. Memorandum R60.9/JB/0516. Reading, UK: Research Department, ECMWF; 2005.
[43] Gunther H, Hasselmann S, Janssen PAEM. The WAM model Cycle 4 (revised version), Deutsch. Klim. Rechenzentrum, Techn. Rep. No. 4. Hamburg, Germany; 1992.
[44] Ardhuin F, Chapron B, Collard F. Observation of swell dissipation across oceans RIDa-1364-2011. Geophys Res Lett 2008;36:L06607.
[45] Cavaleri L, Malanotte-Rizzoli P. Wind wave prediction in shallow water: theory and applications. J Geophys Res 1981;86(No. Cll (10)):961–73.
[46] Törn A, Zilinskas A. Global optimization. New York: Springer Verlag; 2005. p. 255.
[47] Lee BC, Fan YM, Zsu-Hsin Chuang L, Chuen Kao C. Parametric sensitivity analysis of the WAVEWATCH III model. Terr Atmos Ocean Sci 2009;20(2): 425–32.
[48] Tolman HL. Testing of WAVEWATCH III version 2.22 in NCEP's NWW3 ocean wave model suite. NOAA/NWS/NCEP/OMB Technical Note Nr. 214; 2002, 99 pp.
[49] Kahma KK, Calkoen CJ. Reconciling discrepancies in the observed growth of wind generated waves. J Phys Oceanogr 1992;22:1389–405.
[50] Kahma KK, Calkoen CJ. Growth curve observations. In: Komen GJ, Cavaleri L, Donelan M, Hasselmann K, Hasselmann S, Janssen PAEM, editors. Dynamics and modelling of ocean waves. Cambridge University Press; 1994. p. 174–82.
[51] Camus P, Mendez F, Medina R, Cofiño SF. Analysis of clustering and selection algorithms for the study of multivariate wave climate. Coast Eng 2011, http://dx.doi.org/10.1016/j.coastaleng.2011.02.003.
[52] Young IR. Directional spectra of hurricane wind waves. J Geophys Res 2006;111:C08020, http://dx.doi.org/10.1029/2006JC003540.
[53] Zhuo L, Wang A, Guo P. Numerical simulation of sea surface directional wave spectra under typhoon wind forcingExport. J Hydrodyn Ser 2008;B20(6):776–83.
[54] Moon IJ, Ginis I, Hara T, Tolman HL, Wright CW, Walsh EJ. Numerical simulation of sea surface directional wave spectra under hurricane wind forcing. J Phys Ocean 2003;33:1680–760.
[55] Wang C. Variability of the Caribbean low-level jet and its relations to climate. Clim Dyn 2007;29:411–22.
[56] Ruiz MA. Variability Colombia Basin (Caribbean Sea) associated with El Niño-Southern Oscillation, trade winds and local processes; 2011. Thesis submitted as partial requirement for the degree of: Doctor of Engineering - Water Resources [in Spanish].
[57] Appendini CM, Torres-Freyermuth A, Salles P, López-González J, Mendoza ET. Wave climate and trends for the Gulf of Mexico: A 30-yr wave hindcast. J Clim 2014;27:1619–32, http://dx.doi.org/10.1175/JCLI-D-13-00206.1.
[58] Cox AT, Cardone VJ, Swail VR. On the use of the climate forecast system reanalysis wind forcing in ocean response modeling. In: 12th international workshop on wave hindcasting and forcasting & 3rd coastal hazards symposium. 2011. pp. 20, Paper G3.
[59] Kim SU, Kim G, Jeong WM, Jun K. Uncertainty analysis on extreme value analysis of significant wave height at eastern coast of Korea. Appl Ocean Res 2013;41:19–27, http://dx.doi.org/10.1016/j.apor.2013.02.001.
[60] Chawla A, Spindler DM, Tolman HL. Validation of a thirty year wave hindcast using the climate forecast system reanalysis winds. Ocean Modell 2013;70:189–206.
[61] Reguero B, Méndez FJ, Losada IJ. Variability of multivariate wave climate in Latin America and the Caribbean. Global Planet Change 2013;100: 70–84.
[62] Enfield DB, Mayer DA. Tropical Atlantic sea surface temperature variability and its relation to El Niño–Southern Oscillation. J Geophys Res 1997;102(C1):929–45.